



Physikalisch-Technische Bundesanstalt
Braunschweig und Berlin

The following article is hosted by PTB;
DOI: 10.7795/810.20221118 It is provided for personal use only.

Evaluation and Comparison of PIM Measurement Uncertainty using Different Methods

Ahmed Sayegh, Frauke Gellersen, Friederike Stein, and Karsten Kuhlmann

Acknowledgement: The authors would like to thank the Federal Ministry for Digital and Transport, Germany (BMDV) for funding this project (FKZ VB5GFWOPTB) titled “5G-Reallabor in der Mobilitätsregion Braunschweig-Wolfsburg”. Furthermore, authors acknowledge support by the European Metrology Programme for Innovation and Research (EMPIR) Project 20IND03 FutureCom. This project (20IND03) has received funding from the EMPIR programme co-financed by the Participating States and from the European Union’s Horizon 2020 research and innovation programme.

Available at:
<https://doi.org/10.7795/810.20221118>

Evaluation and Comparison of PIM Measurement Uncertainty using Different Methods

Ahmed Sayegh, Frauke Gellersen, Friederike Stein, and Karsten Kuhlmann

Physikalisch-Technische Bundesanstalt (PTB)
Braunschweig, Germany, 38116
Ahmed.Sayegh@PTB.de

ABSTRACT

In this paper, simple methods are proposed for throughout determination of the individual contributions to the uncertainty budget. The power level uncertainty of the two carriers is considered individually and additional uncertainty contributors, namely the drift uncertainty and the connector repeatability, are evaluated. The uncertainty budgets calculated using these two methods are then compared with the uncertainty budget calculated using IEC 62037-1. It is found that the PIM level has a different dependency on each carrier power uncertainty, which results in different contributions from the two carriers to the uncertainty budget. Also, the drift uncertainty is identified as a significant contributor to the uncertainty budget.

INTRODUCTION

THE emerging technologies such as 5G wireless systems and autonomous vehicles are driving the demand for large bandwidth, low latency, and high receiver-sensitivity [1] - [3]. Unfortunately, passive intermodulation (PIM) signals can compromise the receiver sensitivity and thus degrade the performance of the communication systems [3, 4]. Thus, it is of importance to make sure that the RF passive components comply with PIM requirements before deploying them into a communication system.

PIM occurs, when two or more RF signals are mixed in nonlinear contact [5] or nonlinear materials [6]. If the frequency of the generated PIM falls within the operating band of a receiver, it may cause an interference, which may result in decreasing the channel capacity and degrading the performance of the communication system. PIM can be measured with taking into account the associated measurement uncertainty (MU) as described in the IEC 62037-1 standard [7]. However, some contributions are not considered in the uncertainty budget.

In this paper, two methods are pursued for evaluating the sensitivity of PIM level to the carrier power as described in the next section. The measurement setup for measuring PIM of the device under test (DUT) and the procedure for calculating the PIM MU are described in detail in the coming sections. Finally, the results of PIM MU and the uncertainty budget are presented and discussed.

CALCULATION METHODS OF PIM CARRIER POWER SENSITIVITY

Calculation of PIM Sensitivity using Fitted Analytical Model

Several analytical models [8] – [11] are developed for estimating PIM. In [8], the nonlinearity of the DUT is modelled as a polynomial series. The complexity of the polynomial series increases significantly as the number of polynomial terms increases. In many PIM models, the estimated PIM3 has a slope of 3 dB increase for 1 dB increase of both two-tone powers [11]. However, experimental studies reveal that this slope is not always of 3 dB/dB. For better estimation of PIM slope, Henrie [10] has modelled the DUT nonlinearity as a nonlinear resistance connected in series with a linear resistance representing the load as shown in Fig. 1. It is capable to estimate PIM with different slope over carrier power sweep.

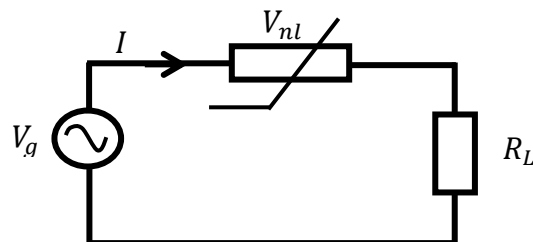


Fig. 1. Equivalent circuit of PIM nonlinear resistor in circuit [10].

where R_L is the terminating load, V_g is the source voltage, I is the current flowing into the circuit and V_{nl} is the voltage across the nonlinear resistor.

The current flowing into the circuit is given as [11], [12]:

$$I = \frac{V_g}{R_L} - \frac{\sqrt[3]{2}(3a_3R_L^3 + 3a_1a_3R_L^4)}{3a_3R_L^3 \left(-27a_3^2R_L^5V_g + \sqrt{4(3a_3R_L^3 + 3a_1a_3R_L^4)^3 + 729a_3^4R_L^{10}V_g^2} \right)^{\frac{1}{3}} + \frac{\left(\sqrt{4(3a_3R_L^3 + 3a_1a_3R_L^4)^3 + 729a_3^4R_L^{10}V_g^2} - 27a_3^2R_L^5V_g \right)^{\frac{1}{3}}}{3\sqrt[3]{2}a_3R_L^3} \quad (1)$$

a_1, a_3 denotes to the fitted coefficients that govern the linear and nonlinear response of the nonlinear resistor respectively.

The computational complexity of Henrie's model is reduced by performing a multiplication of the time domain current signal by a sinusoidal signal with the same frequency of the required harmonic based on the orthogonality technique [11]. The PIM source is modelled as a current source with the load R_L and the signal source resistor R_S in parallel as shown in Fig. 2. The load impedance is characterized in our laboratory while the source impedance is assumed to be 50 Ohms.

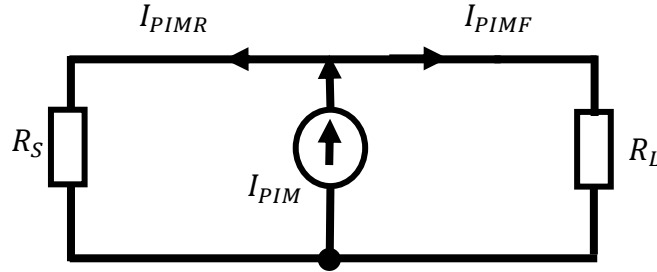


Fig. 2. Equivalent circuit of the forward and reflected PIM current [11].

In [11], the PIM power level is calculated based on the reflected PIM current (I_{PIMR}) only. However, the reflected portion of the forwarded current (I_{PIMF}) from the load back to the source should be considered. Thus, the total PIM current back to the source ($I_{PIMr_{tot}}$) can be expressed as:

$$I_{PIMr_{tot}} = (I_{PIMR} + \rho I_{PIMF}) \quad (2)$$

where ρ is the reflection coefficient of the load.

For calculating the sensitivity of PIM to each carrier power, the model coefficients a_1, a_3 are fitted using two-tone carrier power sweeps versus PIM power measurement data. After fitting the model coefficients (a_1, a_3), the model is employed for estimating PIM level when one carrier power is swept while the other carrier power is fixed. The PIM sensitivity (sen_p) at carrier power p is calculated by dividing the PIM difference at two chosen carrier powers before and after the carrier power p in dBm over the difference between those two chosen carrier powers. Mathematically, it can be expressed as:

$$sen_p = \frac{PIM_{p+\Delta p} - PIM_{p-\Delta p}}{2\Delta p} \quad (3)$$

where $PIM_{p+\Delta p}$ and $PIM_{p-\Delta p}$ are PIM levels in dBm at the successor and predecessor carrier powers around the carrier power p of interest. Δp is the difference in dBm between the carrier power p and the successor or predecessor carrier powers.

Calculation of PIM Sensitivity using Power Sweep Measurement Data

In this work, the model is fitted using PIM measurement data for two-carrier power sweep from 28 dBm to 46 dBm. The fitted model is used for estimating PIM for one-carrier power sweep while the other carrier remains fixed. The sensitivity

of PIM to each carrier power is then calculated based on (3). On the other side, the measurement-based method entails to measure PIM at one-carrier two measurement points, one point before and one point after the operating point of interest. So, only five measurement points are required in total for each operating point of the two carriers to calculate the PIM sensitivity using the measurement-based method. In this study, PIM is measured at several operating points of interest over the power range from 24 dBm to 45 dBm. The Measurement based method depends only on the measurement data and therefore it is considered more reliable than the model method for calculating the PIM sensitivity coefficient.

DESCRIPTION OF PIM MEASUREMENT SETUP

In this study, the PIM is measured based on the reverse PIM measurement setup described in IEC 62037-1. As shown in Fig. 3, the measurement setup consists of scalar PIM site analyzer (PIA) from Rosenberger with 7/16 connector type, Low PIM load and DUT. The DUT is a PIM standard of 4.3-10 connection type from Spinner GmbH with datasheet PIM3 level of -80 dBm at 2.05 GHz. The PIM standard is connected to the analyzer using 4.3-10 to 7/16 adapter. The PIM3 produced by this DUT is measured at different levels of carrier power. First, both carrier-power levels are swept equally from 23 dBm to 46 dBm and the produced PIM3 is recorded.

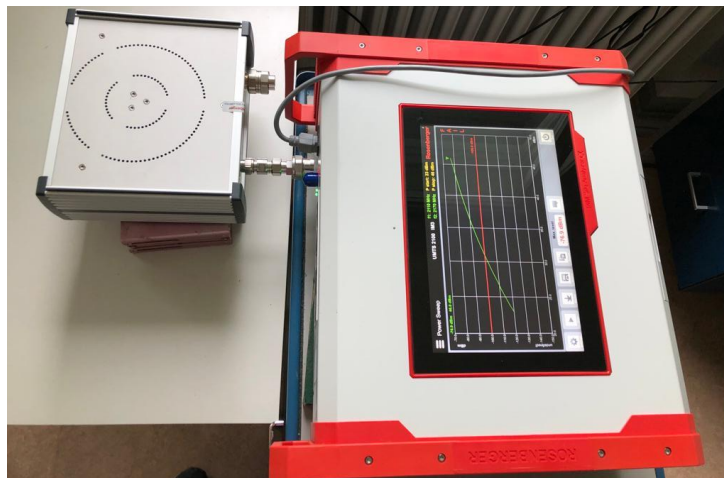


Fig. 3. PIM measurement setup using scalar PIM site analyzer from Rosenberger.

Secondly, the power of carrier 1 is fixed at 43 dBm while the power of carrier 2 is varied from 23 dBm to 46 dBm. Finally, the power of carrier 2 is fixed at 43 dBm while the power of carrier 1 is varied from 23 dBm to 46 dBm.

SCALAR PIM MEASUREMENT UNCERTAINTY

Calculation of PIM MU using IEC 62037-1 Method

Currently, PIM MU is calculated as stipulated in clause 10, IEC 62037-1 based on the following equation [7]:

$$MU = \sqrt{[(\delta A)^2 + (\delta PM)^2 + (\delta SG)^2 + (\delta D)^2]} \quad (4)$$

where δA is the uncertainty of the RF attenuator used for calibrating the transmitted carrier power, δPM is the uncertainty of the power meter used in the calibration, δSG is the uncertainty of the signal generator used for calibrating the receiver and δD is the uncertainty due to self-intermodulation of the measurement system.

Although this approach can provide a fast estimate of PIM MU, it does not provide insight into the actual contribution of each carrier power. Also, the drift and the connector repeatability are not included.

PIM MU using the proposed approaches

The MU is calculated in accordance with the GUM [13] using Matlab [14] and METAS Uncertainty library [15]. The contributors to the uncertainty budget are :

- Carrier power uncertainty

- Attenuator uncertainty
- Power meter uncertainty
- Individual contribution of each carrier
- Receiver uncertainty
- Self-intermodulation associated uncertainty
- Connector repeatability uncertainty
- Drift uncertainty

The process of uncertainty budget calculation is summarized in Fig. 4.

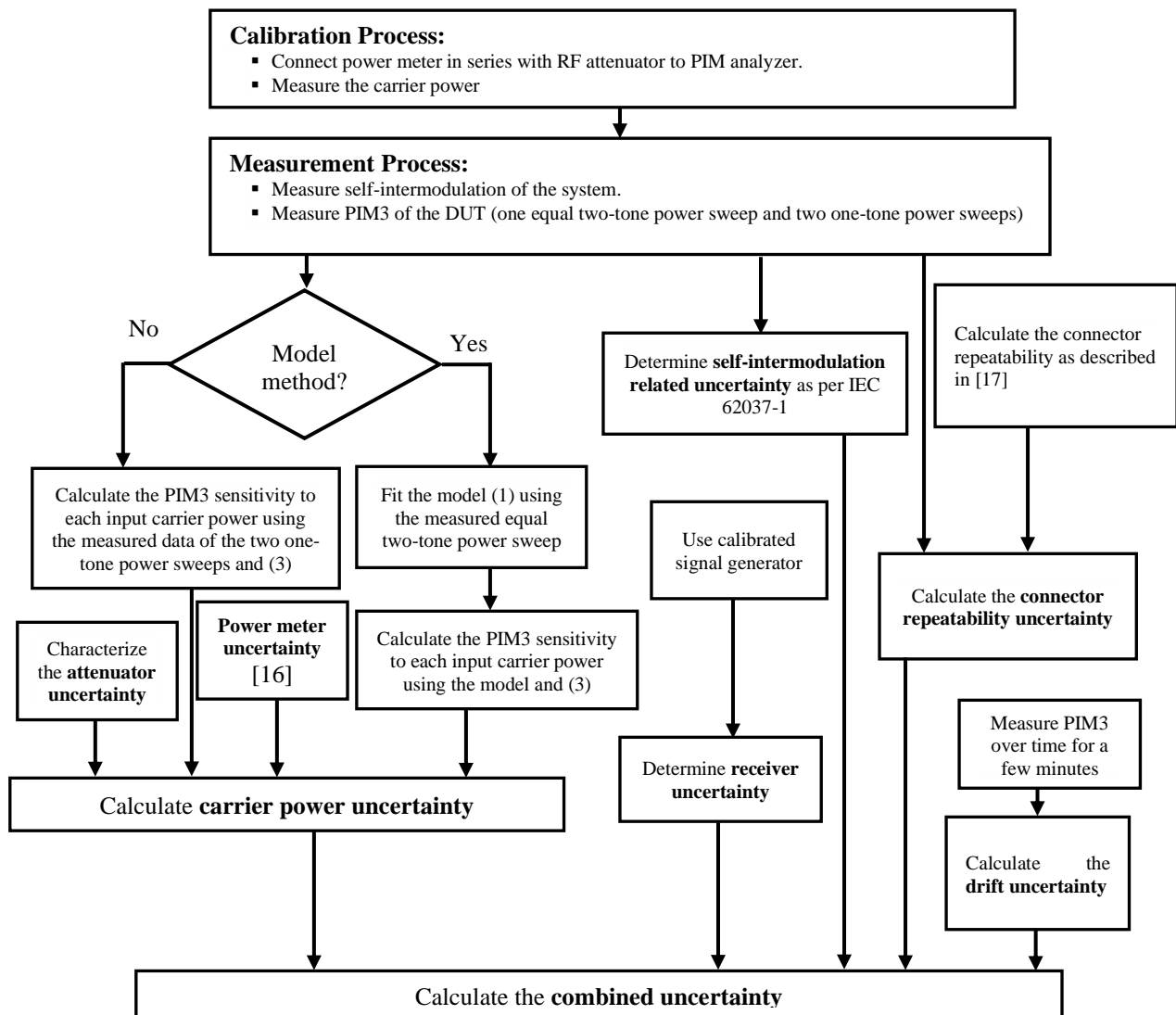


Fig. 4. calculation process of PIM MU.

PIM3 carrier power uncertainty: Carrier power uncertainty is the combination of power meter uncertainty and the attenuator uncertainty. The sensitivity of PIM3 to each input carrier is evaluated based on (3) and thus the uncertainty budget provides information about the impact of each carrier on PIM uncertainty. The PIM sensitivity is calculated then using both the model method and the measurement method. The carrier power uncertainty results are presented below in the result and discussion Section.

- **Power meter uncertainty:** The uncertainty of the power measured by the power meter is calculated based on the relative uncertainty in the datasheet given by the manufacturer. In this work, a R&S NRP33T power meter is used for determining the transmitted carrier power. The relative uncertainty of this power meter is 0.01dB [16].

- **RF attenuator uncertainty:** The RF attenuator is used to attenuate the carrier power before delivering it to the power sensor since the sensor is unable to measure power higher than +20 dBm. In this study, a 30 dB RF-attenuator is used during the calibration of each carrier power. This RF attenuator is characterized by measuring the scattering parameters at each carrier frequency (2.11 GHz for carrier 1 and 2.17 GHz for carrier 2).

Receiver uncertainty and self-intermodulation associated uncertainty: The receiver uncertainty and self-intermodulation associated uncertainty are determined as described in IEC 62037-1.

Connector repeatability uncertainty: The contribution of the connector repeatability uncertainty to the uncertainty budget depends on the connector type. In this work, the repeatability of 4.3-10 connector type is evaluated in accordance with EURAMET guidelines on the evaluation of Vector Network Analyzers (VNA) [17]. For this purpose, several measurements of scattering parameters in different azimuthal positions of 4.3-10 short calibration standard. The difference between the maximum and the minimum value of the measured estimate is taken as the connector repeatability, and it is less than -60 dB at 2.1 GHz as shown in Fig. 5. The connector repeatability uncertainty is then calculated through multiplying the connector repeatability in linear by the measured PIM3 power level in watt.

Drift uncertainty: In this work, two PIM standards are used to investigate the drift; namely a PIM standard of -80 dBm (at 2 x 43 dBm) from Spinner GmbH and a PIM standard of -80 dBm (at 2 x 43 dBm) from HUBER+SUHNER. The 43 dBm power level is chosen because it is the point where the PIM measurement is conducted. The drift is a combination of thermal drift, DUT drift and PIM measurement system drift. It is evaluated by measurement of PIM3 over time. The maximum difference between PIM3 over time (PIM3(t)) and PIM3 at time equal zero (PIM3(t0)) is used to determine the drift envelope. First, the drift is measured for several minutes in order to identify the point where PIM3 becomes stable. However, it is found that PIM level keeps increasing or decreasing over time based on the characteristics of the DUT as shown in Fig. 6. Therefore, it is very feasible and practical to calculate the drift within a defined time frame. In this paper, the drift is calculated by measuring PIM within the first minute and then the maximum deviation is determined to be 0.08 dBm. Taking into account the different responses of DUTs, the drift uncertainty is estimated to be ± 0.1 dBm.

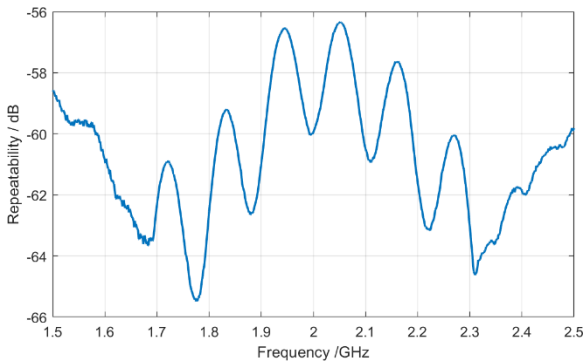


Fig. 5. Characterized repeatability of 4.3-10 connector standards.

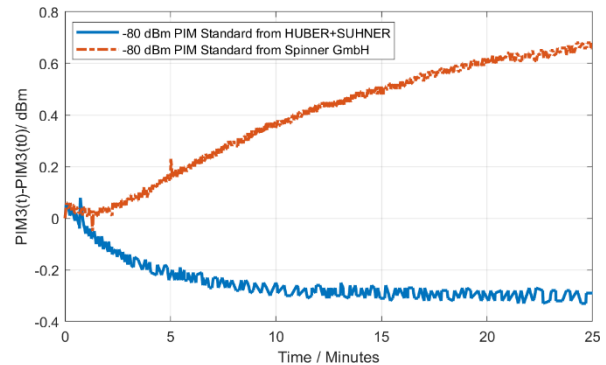


Fig. 6. Drift measurements using -80 dBm PIM standards.

RESULTS AND DISCUSSION

Results of PIM3 Sensitivity Calculation

Fig. 7 shows the measured power of lower IM3 for two-carrier power sweep from 23 dBm to 46 dBm. The frequencies of carrier 1 and carrier 2 are 2.11 GHz and 2.17 GHz respectively. The powers of the two carriers (displayed on x-axis) are measured and corrected using a power meter and a characterized RF attenuator. For the first case (Fig. 7 blue crosses), the two carriers are swept from 23 dBm to 46 dBm. For the second case (Fig. 7 red stars), carrier 2 power is fixed at 43 dBm while carrier 1 power is swept from 23 dBm to 46 dBm. For the third case (Fig. 7 green diamond), carrier 1 power is fixed at 43 dBm and carrier 2 power is swept from 23 dBm to 46 dBm. It is observed that the measured PIM3 for carrier 2 power sweep (Fig. 7 green diamond) increases steadily in the low power range and tends to slightly increase for high power range so carrier 2 has less impact on PIM at high power range.

Fig. 7 shows that the PIM3 power has a stronger dependency on carrier 1 power than carrier 2 power. Indicating that, the lower frequency PIM3 is more sensitive to the variation of carrier 1 power than to the variation of carrier 2 power. The

sensitivity coefficients (slope) [13] of PIM3 to the swept carrier power is calculated using both the model and the measurement methods. For carrier 1 power sweep, the model underestimates the PIM3 sensitivity compared to the measurement method at the low power range. Both methods reveal that PIM3 has different sensitivity dependent on the considered carrier. For carrier 2 power sweep, the sensitivity coefficients calculated using the model are in a good agreement with that calculated using the measurement method as depicted in Fig. 8 (green squares).

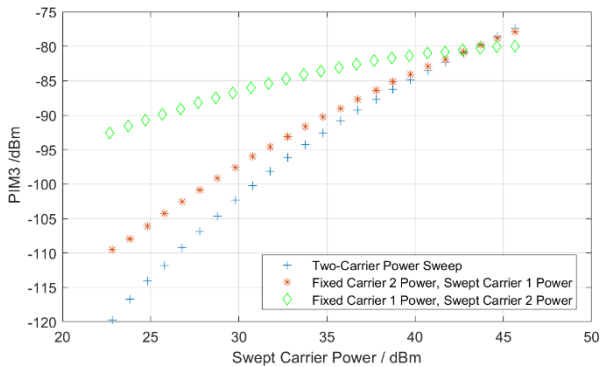


Fig. 7. Measured PIM3 versus power sweep produced from -80 dBm PIM standard from Spinner GmbH.

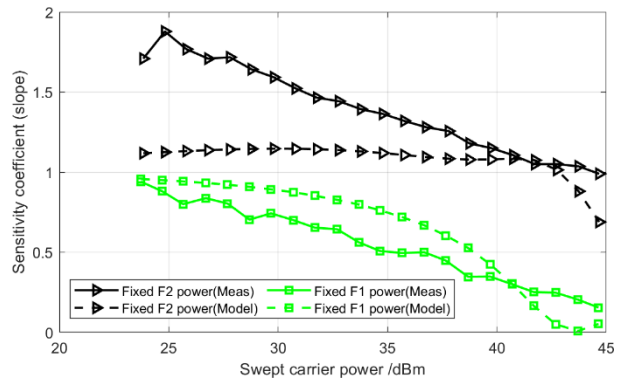


Fig. 8. Lower-PIM3 sensitivity to one carrier power while the other carrier is fixed at 43 dBm.

Results of PIM3 Uncertainty

The PIM3 uncertainty increases rapidly as the carrier power decreases as shown in Fig. 9. The PIM3 power becomes very low when the carrier power decreases and consequently the self-intermodulation related uncertainty becomes large due to the small difference between PIM3 power level and self-intermodulation power level. Fig. 9 shows that the MU results obtained using IEC 62037-1 is less than the uncertainty results obtained using the proposed methods particularly in the low power range. These uncertainties are calculated at 95% coverage interval with coverage factor ($K=2$). This behavior is expected since IEC62037-1 does not account for the drift and connector repeatability.

On the other hand, the uncertainty results obtained from the model are in a good agreement with the uncertainty results obtained using the measurement as portrayed in Fig. 9. However, there is nearly perfect match between uncertainties obtained from the model and the measurement results. The model method is fast to get the result but it is less accurate compared to the measurement. Therefore, the model is a good tool to be used when the approximated uncertainty is tolerable.

Results of PIM3 Uncertainty Budget

The uncertainty budget of PIM3 is calculated using all the aforementioned methods. Fig. 10 shows the uncertainty budget using the IEC 62037-1 approach. The self IM contributes significantly to the budget when the carrier power is lower than around 33 dBm. However, the carrier power tends to be the main contributor to the budget when the carrier power is more than around 33 dBm.

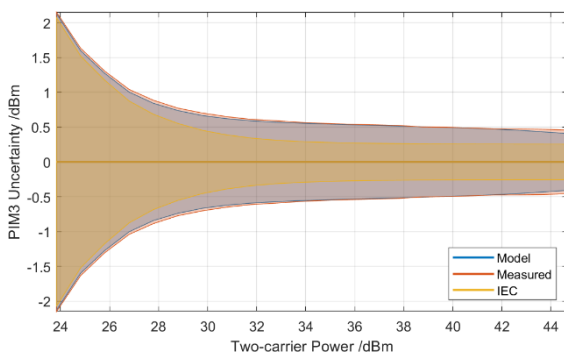


Fig. 9. PIM3 uncertainty calculated using the proposed methods and the IEC 62037-1 method.

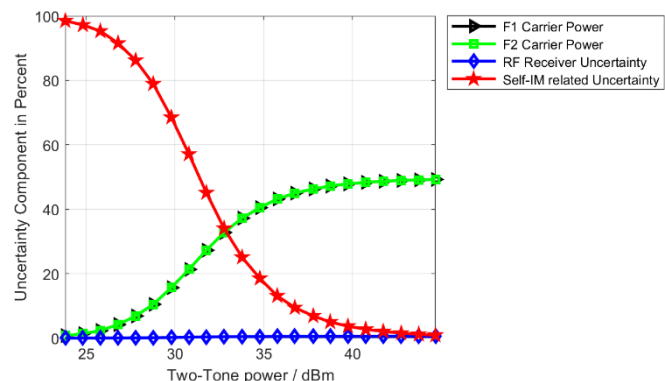


Fig. 10. PIM3 uncertainty budget using the IEC 62037-1 method.

Since the PIM sensitivity to each carrier power is not taken into the account in IEC 62037-1, the uncertainty contributions of carrier 1 power and carrier 2 power to the budget are the same as shown in Fig. 10. For both measurement and model-based methods, it is found that carrier 1 and carrier 2 have different contributions to the budget as depicted in Fig. 11 and Fig. 12 respectively. Carrier 1 power contributes significantly more to the budget than carrier 2 power and these contributions tend to decrease with increasing carrier power. So, it is observed that carrier 1 power is responsible about almost 60% of the budget when the two-tone powers are 43 dBm while carrier 2 power contributes with around 20% of the budget. The self-intermodulation related uncertainty is the dominant contributor to the budget at the lower carrier-power range. The drift uncertainty is the third significant contributor to the uncertainty budget. The drift contribution (around ± 0.1 dB as specified before) is taken as constant value over the whole power range. However, the drift percentage in the overall uncertainty budget, as shown in Fig. 11 and Fig. 12, increases as the carrier power increases because of the contributions from carrier power and self-intermodulation decreases.

Although the results of this evaluation show the importance of considering the drift and the PIM sensitivity to each carrier power into the budget, further evaluation would be carried out to include the mismatch errors and their uncertainty into the uncertainty budget. Also, the receiver contribution would be thoroughly investigated in the future and the drift subcomponents would be individually investigated.

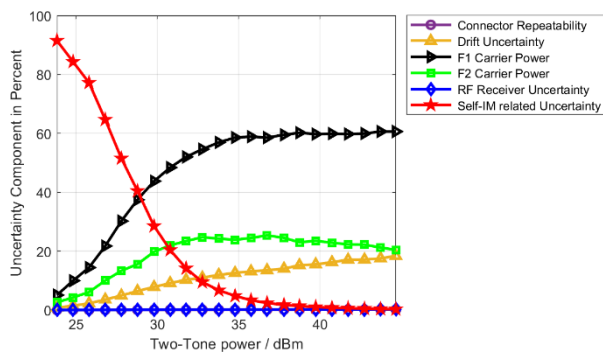


Fig. 11. PIM3 uncertainty budget using the measurement method.

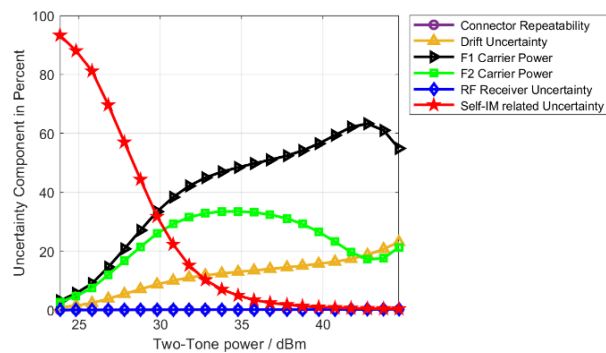


Fig. 12. PIM3 uncertainty budget using the model-based method.

CONCLUSION

In this paper, two approaches are proposed for calculating the PIM MU budget based on an analytical model and measurement data. The results obtained from the model are not in perfect agreement with those results obtained using measurement method. However, the model-based method is a suitable option when the approximated uncertainty is tolerable. It is recommended to use the measurement-based method to obtain accurate uncertainty budget for scalar PIM measurement results. The PIM3 level has a different sensitivity to each carrier power level, and this leads to different contributions to the total uncertainty budget. The lower PIM3 is more sensitive to carrier 1 power, making it a significant contributor to the uncertainty budget. This evaluation shows that the drift contributes significantly to the uncertainty budget, while the connector repeatability has a minor impact onto the budget. The uncertainty calculated using IEC 62037-1 is smaller than that calculated using the proposed methods, because IEC 62037-1 does omit some sources of MU. In future, the PIM uncertainty budget would include the mismatch uncertainty of the components used during the calibration and measurement processes.

ACKNOWLEDGMENT

The authors would like to thank the Federal Ministry for Digital and Transport, Germany (BMDV) for funding this project (FKZ VB5GFWOPTB) titled “5G-Reallabor in der Mobilitätsregion Braunschweig-Wolfsburg”. Furthermore, authors acknowledge support by the European Metrology Programme for Innovation and Research (EMPIR) Project 20IND03 FutureCom. This project (20IND03) has received funding from the EMPIR programme co-financed by the Participating States and from the European Union’s Horizon 2020 research and innovation programme.

REFERENCES

- [1] S. Mumtaz, J. M. Jornet, J. Aulin, W. H. Gerstacker, X. Dong, and B. Ai, “Terahertz communication for vehicular networks”, *IEEE Transactions on Vehicular Technology*, vol. 66, no. 7, 2017.

- [2] D. U. C. Delgado, C. A. Gutierrez, and O. Caicedo, "5G and beyond: Past, Present and Future of the Mobile Communications", *IEEE Latin America Transactions*, vol. 19, no. 10, pp. 1702–1736, 2021.
- [3] R. Butler, "Advanced wireless services emphasize the need for better PIM control", *White Paper CommScope*, 2017.
- [4] D. S. Kozlov, A. P. Shityov, A. G. Schuchinsky, and M. B. Steer, "Passive intermodulation of analog and digital signals on transmission lines with distributed nonlinearities: Modelling and characterization", *IEEE Transactions on microwave theory and techniques*, vol. 64, no. 5, pp. 1383–1395, 2016.
- [5] P. L. Lui, "Passive intermodulation interference in communication systems", *Electronics Communication Engineering Journal*, vol. 2, pp. 109–118, June 1990.
- [6] X. Chen and Y. He, "Reconfigurable Passive Intermodulation Behavior on Nickel-Coated Cell Array", *IEEE Transactions on Electromagnetic Compatibility*, vol. 59, pp. 1027–1034, Aug 2017.
- [7] International Electrotechnical Commission, "Passive RF and microwave devices, intermodulation level measurement part 1: General requirements and measuring methods", 2012.
- [8] J. C. Pedro and N. B. Carvalho, *Intermodulation Distortion in Microwave and Wireless Circuits*. Artech House, 2003.
- [9] J. Henrie, A. Christianson, and W. J. Chappell, "Prediction of Passive Intermodulation from Coaxial Connectors in Microwave Networks", *IEEE Transactions on Microwave Theory and Techniques*, vol. 56, pp. 209–216, Jan. 2008.
- [10] J. Henrie, A. Christianson, and W. J. Chappell, "Engineered passive nonlinearities for broadband passive intermodulation distortion mitigation", *IEEE microwave and wireless components letters*, vol. 19, no. 10, pp. 614–616, 2009.
- [11] M. Petek, "Modelling of passive intermodulation in RF systems", Master's thesis, KTH Royal Institute Of Technology, 2020.
- [12] J. Henrie, A. Christianson, and W. J. Chappell, "Linear-nonlinear interactions effect on the power dependence of nonlinear distortion products", *Applied Physics Letters*, vol. 94, no. 11, p. 114101, 2009.
- [13] Working Group 1 of the Joint Committee for Guides in Metrology, *Evaluation of measurement data - Guide to the expression of uncertainty in measurement*. JCGM, Sept. 2008.
- [14] MATLAB, version 9.8.0.1417392 (R2020a). Natick, Massachusetts: The MathWorks Inc., 2020.
- [15] M. Wollensack, "METAS UnLib Matlab - User Reference v2.5.3", Federal Institute of Metrology METAS.
- [16] Rohde & Schwarz, *NRP33T Thermal Power Sensors User Manual*, 2021.
- [17] M. Zeier, D. Allal, and R. Judaschke, "Guidelines on the evaluation of Vector Network Analysers (VNA)", 2018.